

# Niobium Complexes in Fluoride Melts

V. VAN, J. MADEJOVÁ, A. SILNÝ, and V. DANĚK

*Institute of Inorganic Chemistry, Slovak Academy of Sciences, SK-842 36 Bratislava*

Received 15 July 1999

Complex formation and redox chemistry of the niobium complex in fluoride melts has been studied by cyclic voltammetry and chronopotentiometry. The X-ray powder diffraction analysis and IR spectroscopy was used to clarify the complex formation in the high oxidation states of niobium metal. Two-step reversible diffusion-controlled mechanism in the melt at 750 °C  $\text{Nb(V)} \rightarrow \text{Nb(IV)} \rightarrow \text{Nb(0)}$  was confirmed. In the presence of oxide ions in fluoride melts niobiumoxyfluoro complexes are formed. At low oxide concentration mono-oxyfluoro complexes have the form of  $[\text{Nb(V)OF}_5]^{2-}$ . With the  $n_{\text{O}}:n_{\text{Nb(V)}}$  ratio higher than 0.7 the complex changes to the  $[\text{Nb(V)OF}_6]^{3-}$  one. The ligand displacement of the niobium fluoro complexes to the mono-oxyfluoro complexes is not complete and the conversion degree was found to be 0.7. Free oxide ions cause di-oxyfluoro complexes formation that both oxyfluoro complexes coexist despite the low oxide concentration in the melt. The diffusion coefficient of oxyfluoro complexes in fluoride melts depends on the  $n_{\text{O}}:n_{\text{Nb(V)}}$  ratio in the melts. With the  $n_{\text{O}}:n_{\text{Nb(V)}}$  ratio up to 0.7 there is no change in the diffusion coefficient of the mono-oxyfluoro complex. The coefficient strongly increases in the ratio interval 0.7–0.9 and then again decreases.

Demand for niobium has increased during the last decades because of its high technology applications such as in nuclear reactors, as materials for aerospace industry, superconductors, catalysis, *etc.* For these special applications niobium should be of a highest purity.

Molten salt electrolysis is an alternative process for niobium production to classical thermal reduction and provides niobium with required purity. The necessity to know the details of both complex formation and redox chemistry of the species present in the melts is of prime importance in order to optimize the process. In our investigation,  $\text{LiF—KF}$  and  $\text{LiF—NaF}$  melts have been used as solvent for niobium salts. To study the redox chemistry, electrochemical methods, mainly cyclic voltammetry has been used. Chronopotentiometry was used for obtaining quantitative data on the system. The X-ray powder diffraction analysis and IR spectroscopy was used to clarify the complex formation in the high oxidation states of niobium metal.

## EXPERIMENTAL

The alkali fluorides ( $\text{LiF}$ , pure, Ubichem,  $\text{KF}$ , anal. grade, Lachema, and  $\text{NaF}$ , anal. grade, Lachema) used in the experiments were dried first for 48 h in vacuum at *ca.* 200 °C, then for 24 h in a furnace at 450 °C under an argon atmosphere. The niobium oxyfluorides were prepared by means of controlled additions of  $\text{Na}_2\text{O}$  (97 %, Aldrich) or  $\text{K}_2\text{O}$  formed *in situ* by decompo-

sition of  $\text{K}_2\text{CO}_3$  (anal. grade, Lachema) added to the melts.  $\text{K}_2\text{NbF}_7$  was prepared from  $\text{Nb}_2\text{O}_5$  (99.9 %, Fluka) according to the method of *Sakawa* and *Kuroda* [1]. The more detailed description of this procedure is given in [2]. All operations during the melt preparation, manipulation, and weighting of chemicals were performed in a glove box under dry nitrogen.

The samples of the melts for X-ray diffraction analysis and IR spectroscopy investigation have been taken from the melts after voltammetric measurement. The samples were taken using a graphite rod immersed into the melts and quickly taken off the melt. Such a procedure provided samples of the quenched melt with possibly unchanged structure [3]. Due to the experimental difficulties to keep the samples under dry atmosphere during sampling and manipulation there was no further special adjustment applied to dehydrate the samples after quenching.

The X-ray powder diffraction patterns of the samples were measured at room temperature in the range 6–60° ( $2\theta$ ) with steps of 1°. The measurements were done on Philips PW1349/30 diffractometer using  $\text{CuK}\alpha$  radiation. Identification of the present phases was done using the PDF-2 International Centre for Diffraction Data database. The infrared spectra were obtained using a FTIR spectrometer Nicolet Magna 750 equipped with DTGS detector. For each sample 128 scans were recorded in the 400–4000  $\text{cm}^{-1}$  spectral range with a resolution of 4  $\text{cm}^{-1}$ . Solidified melts were analyzed by KBr pressed disc technique, which

## RESULTS AND DISCUSSION

## Cyclic Voltammetric Study

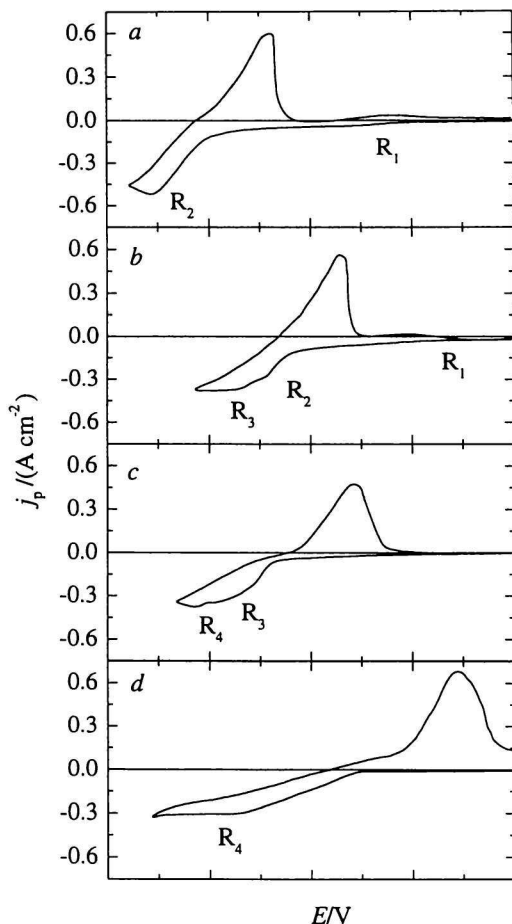


Fig. 1. Cyclic voltammograms of  $\text{K}_2\text{NbF}_7$  in LiF—KF equimolar melts with initial  $\text{K}_2\text{NbF}_7$  concentration  $c(\text{Nb(V)}) = 57.1 \text{ mol m}^{-3}$ ,  $\nu = 0.36 \text{ V s}^{-1}$ , and various amounts of added  $\text{K}_2\text{O}$  at  $700^\circ\text{C}$ . Platinum quasi-reference electrode. a)  $n_{\text{O}}:n_{\text{Nb}} = 0$ , b)  $n_{\text{O}}:n_{\text{Nb}} = 0.6$ , c)  $n_{\text{O}}:n_{\text{Nb}} = 1$ , d)  $n_{\text{O}}:n_{\text{Nb}} = 1.5$ .

is the most widely used method for routine transmission measurements of solid samples. 2 mg of the sample were dispersed in 200 mg of KBr to give a uniform mixture, which after pressing gave a 13 mm disc. While KBr is hygroscopic, contamination of the melts by water could not be excluded. On the other hand, the absorption bands of adsorbed water (near  $1600 \text{ cm}^{-1}$  and  $3400 \text{ cm}^{-1}$ ) do not overlap the spectral region important for niobiumoxyfluoro complexes identification ( $400\text{--}1000 \text{ cm}^{-1}$ ). The assignment of the bands follows the procedure described in [4–10].

Voltammetric and chronopotentiometric study was carried out under argon atmosphere in a closed furnace at  $700^\circ\text{C}$  and  $750^\circ\text{C}$  [2]. The three-electrode system was used. Potential was measured against platinum quasi-reference electrode. The platinum wire of 1 mm in diameter was used as working electrode while a platinum crucible containing 25 g of melts was used as counter electrode [2].

Fig. 1 shows typical cyclic voltammograms in LiF—KF— $\text{K}_2\text{NbF}_7$  melt with an initial concentration of  $\text{K}_2\text{NbF}_7$   $c(\text{Nb(V)}) = 57.1 \text{ mol m}^{-3}$ , recorded at  $700^\circ\text{C}$ , the scanning rate of  $0.36 \text{ V s}^{-1}$  with different concentration of oxide ions. The first voltammogram (Fig. 1a) shows that the electrochemical reduction of Nb(V) apparently proceeds in two steps. The first wave ( $R_1$ ) at  $-0.24 \text{ V}$  is followed by a sharp peak ( $R_2$ ) at  $-0.87 \text{ V}$ . These steps were attributed to the reduction of Nb(V) to Nb(IV) and of Nb(IV) to Nb(0), respectively [2].

When oxide ions were added, a ligand displacement reaction took place. In Fig. 1b a new reduction peak ( $R_3$ ) was observed at a potential about 100 mV more negative than  $R_2$ . In the melts with oxide ions the reduction peak potentials were shifted towards positive values. The reason for this was most probably the change in the platinum quasi-reference electrode potential with the presence of oxide ions in the melt. Transformation is complete when the ratio  $n_{\text{O}}:n_{\text{Nb(V)}} = 1$ . At this ratio a further reduction peak  $R_4$  occurs at a potential about 80 mV more negative than  $R_3$ . The reduction peaks  $R_3$  and  $R_4$  have been ascribed to the reduction of the mono- and di-oxyfluoro complexes of Nb(V) ions, respectively [2, 5]. These results are in accordance with the results of the X-ray powder diffraction analysis and the IR spectroscopic study of the melts.

Fig. 2 shows typical cyclic voltammograms in

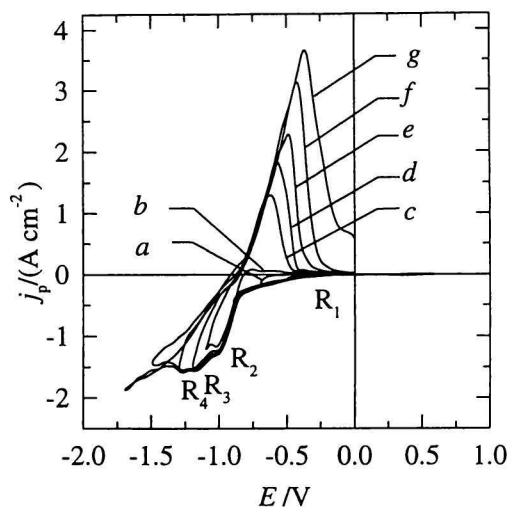


Fig. 2. Voltammograms in the system LiF—KF— $\text{K}_2\text{NbF}_7$ — $\text{K}_2\text{O}$  at  $720^\circ\text{C}$ .  $c(\text{Nb(V)}) = 475 \text{ mol m}^{-3}$ ;  $n_{\text{O}}:n_{\text{Nb(V)}} = 0.5$ ;  $\nu = 1.0 \text{ V s}^{-1}$ ; switching potential  $-E_{\lambda}/V$ : a) 0.7, b) 0.9, c) 1.1, d) 1.2, e) 1.3, f) 1.5, g) 1.7. Platinum quasi-reference electrode.

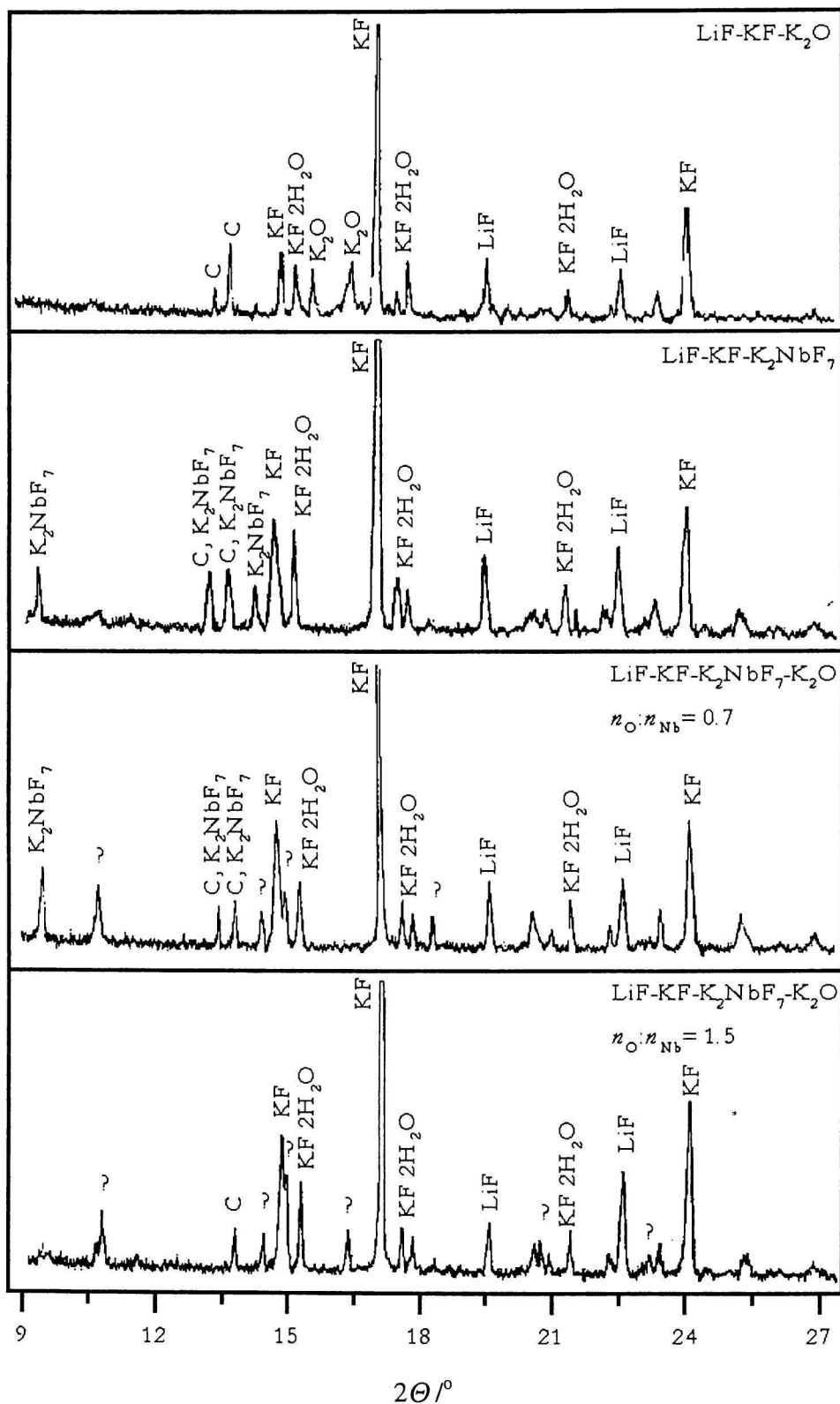


Fig. 3. X-Ray diffraction pattern for samples obtained during the voltammetric measurements with initial concentration of  $K_2NbF_7$   $c(Nb(V)) = 570.46 \text{ mol m}^{-3}$  at  $700^\circ\text{C}$ .

LiF—KF— $K_2NbF_7$ — $K_2O$  melt with the initial concentration of  $K_2NbF_7$   $c(Nb(V)) = 475 \text{ mol m}^{-3}$

and the ratio  $n_O:n_{Nb(V)} = 0.5$ , recorded at  $720^\circ\text{C}$ , the scanning rate of  $1 \text{ V s}^{-1}$ , and different switch-

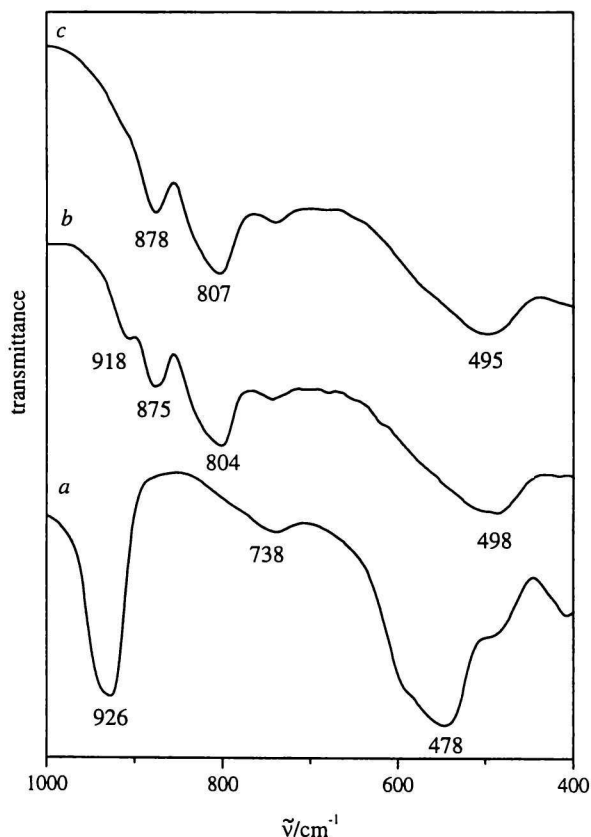


Fig. 4. Infrared spectra of quenched LiF—KF—K<sub>2</sub>NbF<sub>7</sub>—K<sub>2</sub>O melts with initial concentration of K<sub>2</sub>NbF<sub>7</sub>  $c(\text{Nb(V)}) = 570.46 \text{ mol m}^{-3}$  at 700 °C. a)  $n_{\text{O}}:n_{\text{Nb(V)}} = 0.2$ , b)  $n_{\text{O}}:n_{\text{Nb(V)}} = 1$ , c)  $n_{\text{O}}:n_{\text{Nb(V)}} = 1.5$ .

ing potentials. The voltammograms show all four reduction peaks. The simultaneous appearance of R<sub>4</sub> and R<sub>2</sub> indicates that the conversion of fluoro complexes to mono-oxyfluoro complexes does not proceed completely and that further addition of free oxide ions causes further conversion of mono-oxyfluoro complexes to di-oxyfluoro complexes.

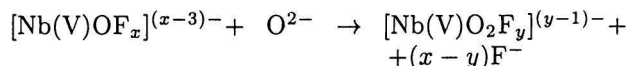
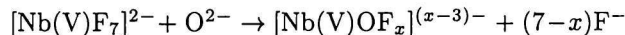
Fig. 3 shows the X-ray powder diffraction patterns of samples obtained during voltammetric measurements. New peaks were observed when oxide was added to the melts. At the ratio  $n_{\text{O}}:n_{\text{Nb(V)}} = 1.5$  K<sub>2</sub>NbF<sub>7</sub> seems already not to be present. New peaks represent the niobium oxyfluoro complexes, which were reported at the cyclic voltammetric study.

### Infrared Spectra

The characteristic vibrations of niobiumoxyfluoro complexes were found in the 400–1000 cm<sup>-1</sup> region. Fig. 4 shows infrared spectra of K<sub>2</sub>NbF<sub>7</sub> dissolved in equimolar LiF—KF melt with  $c(\text{Nb(V)}) = 570 \text{ mol m}^{-3}$  and various  $n_{\text{O}}:n_{\text{Nb(V)}}$  ratio at 700 °C. Since some oxide and water contamination during the sampling is unavoidable, none of the spectra represent oxygen-free

niobium fluoride species. The IR spectrum of the sample with  $n_{\text{O}}:n_{\text{Nb(V)}} = 0.2$  shows a sharp band at 926 cm<sup>-1</sup> which is characteristic of Nb=O stretching vibration in [Nb(V)OF<sub>5</sub>]<sup>2-</sup> (Fig. 4a). The absorption band at 738 cm<sup>-1</sup> is supposed to correspond to the vibrations of bridging oxygen—niobium bonds. The broad complex band near 550 cm<sup>-1</sup> consists of several overlapping components due to Nb—F vibrations of both [Nb(V)OF<sub>5</sub>]<sup>2-</sup> and [Nb(V)F<sub>7</sub>]<sup>2-</sup> complexes. With addition of oxide up to the ratio  $n_{\text{O}}:n_{\text{Nb(V)}} = 1$  a pronounced decrease of the intensity and a shift of the Nb=O band to 918 cm<sup>-1</sup> is observed, which indicates a presence of [Nb(V)OF<sub>6</sub>]<sup>3-</sup> in the melt (Fig. 4b). Moreover, two new bands at 875 cm<sup>-1</sup> and 804 cm<sup>-1</sup>, assigned to O—Nb—O stretching vibrations in di-oxyfluoro complexes are observed. The Nb—F band is shifted to 498 cm<sup>-1</sup>, position found for [Nb(V)O<sub>2</sub>F<sub>y</sub>]<sup>(y-1)-</sup>. No Nb=O band near 920 cm<sup>-1</sup> in the spectrum of the melt with oxide content corresponding to the ratio  $n_{\text{O}}:n_{\text{Nb(V)}} = 1.5$  indicates any or negligible amount of double bonds (Fig. 4c). Absorptions at 878 cm<sup>-1</sup>, 807 cm<sup>-1</sup>, and 495 cm<sup>-1</sup> are consistent with O—Nb—O and Nb—F stretching vibrations in di-oxyfluoro complex [Nb(V)O<sub>2</sub>F<sub>y</sub>]<sup>(y-1)-</sup>.

The IR spectra indicate a transformation of [Nb(V)F<sub>7</sub>]<sup>2-</sup> through [Nb(V)OF<sub>x</sub>]<sup>(x-3)-</sup> to [Nb(V)O<sub>2</sub>F<sub>y</sub>]<sup>(y-1)-</sup> with increasing oxide content in the melts. The ligand displacement reactions can be described as



where  $x$  could be 5 and 6 and  $y$  may take a value of 2, 3 or 4 [5, 10].

It is well known that with increasing  $n_{\text{O}}:n_{\text{F}}$  ratio in the melts the activity of fluoride ions decreases. In our experiments the  $n_{\text{O}}:n_{\text{F}}$  ratio increases with the increasing oxide amount added, the mono-oxyfluoro complex most probably establishes as [Nb(V)OF<sub>5</sub>]<sup>2-</sup>. Thus, the experimentally determined transition of [Nb(V)OF<sub>5</sub>]<sup>2-</sup> to [Nb(V)OF<sub>6</sub>]<sup>3-</sup> with increasing oxide concentration in the melt is not due to the activity of fluoride ions in the melts. The formation of [Nb(V)OF<sub>6</sub>]<sup>3-</sup> in the LiF—KF melt was found previously, too [6]. To explain the reason for the nonclassical behaviour of mono-oxyfluoro complexes there is needed another work, which is intended to deal with the niobium complexes structure.

### Chronopotentiometric Study

Fig. 5 shows the chronopotentiograms of LiF—NaF—K<sub>2</sub>NbF<sub>7</sub> melt at 750 °C with different initial concentration of K<sub>2</sub>NbF<sub>7</sub> and different amounts of Na<sub>2</sub>O added. In the absence of oxide ions, only one

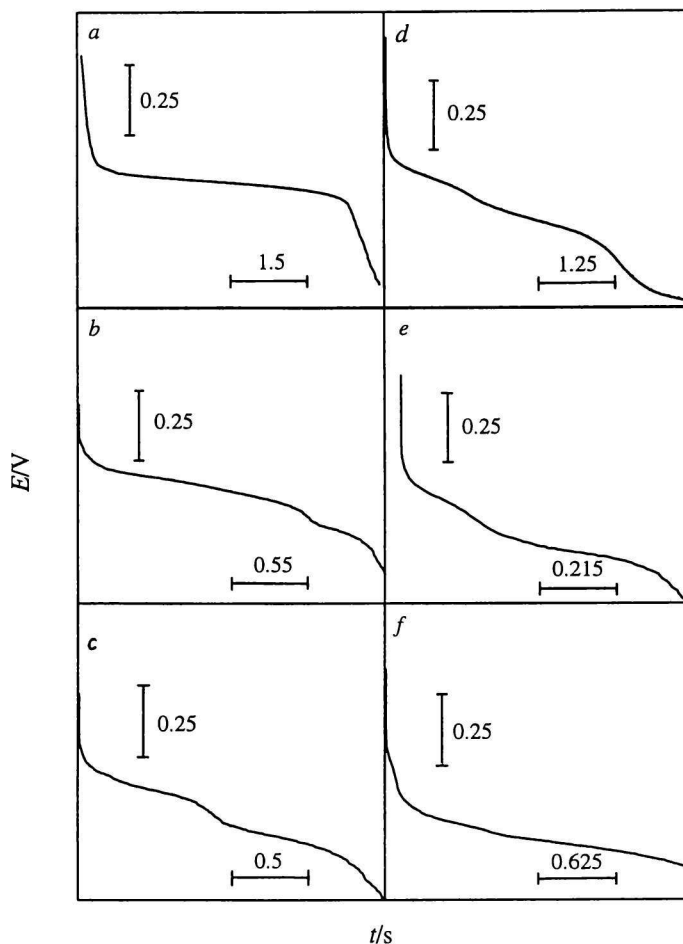


Fig. 5. Chronopotentiograms in melts with different initial concentrations of  $\text{K}_2\text{NbF}_7$  and various amount of added  $\text{Na}_2\text{O}$  at  $750^\circ\text{C}$ . Platinum working electrode. a)  $n_{\text{O}}:n_{\text{Nb(V)}} = 0$ , b)  $n_{\text{O}}:n_{\text{Nb(V)}} = 0.23$ , c)  $n_{\text{O}}:n_{\text{Nb(V)}} = 0.62$ , d)  $n_{\text{O}}:n_{\text{Nb(V)}} = 0.67$ , e)  $n_{\text{O}}:n_{\text{Nb(V)}} = 0.8$ , f)  $n_{\text{O}}:n_{\text{Nb(V)}} = 1$ .

wave corresponding to the reduction of Nb(IV) to Nb(0) was observed. In the presence of oxide ions a new wave appeared at the potential around  $-1.06$  V. Since only niobium ions are present as the electrochemical active species in the system and the reduction potential of alkali ions is far more negative than  $-1.7$  V, the wave can be ascribed to the reduction of some niobium species. With increasing  $n_{\text{O}}:n_{\text{Nb(V)}}$  ratio the transition time of the second wave increases compared to that of the first wave. The appearance of the second reduction wave simultaneously with the decreased transition time of the first wave indicates that a ligand displacement reaction under formation of a new complex may take place. Analysis of the first wave resulted in obtaining reversible diffusion-controlled reduction of Nb(IV) to Nb(0).

Assuming ligand displacement is complete, the diffusion coefficients of niobiumfluoro complexes calculated from the chronopotentiometric data (Table 1) are very high compared to the values calculated for the system without oxide ions ( $D_{\text{Nb(V)}} = 3.2 \times 10^{-5} \text{ cm}^2 \text{ s}^{-1}$  [2]). For example, for the system with initial

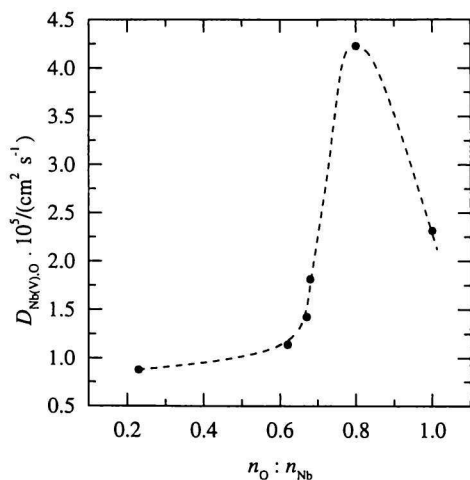
concentration of  $\text{K}_2\text{NbF}_7$   $c(\text{Nb(V)}) = 114 \text{ mol m}^{-3}$ ,  $n_{\text{O}}:n_{\text{Nb(V)}} = 0.67$ , and at current density  $j = 1111 \text{ A m}^{-2}$  they are  $D_{\text{Nb(V)}} = 8.5 \times 10^{-5} \text{ cm}^2 \text{ s}^{-1}$  and  $D_{\text{Nb(V),O}} = 0.7 \times 10^{-5} \text{ cm}^2 \text{ s}^{-1}$ . Comparing with the diffusion coefficient obtained in the system without oxide ions ( $D_{\text{Nb(V)}} = 3.2 \times 10^{-5} \text{ cm}^2 \text{ s}^{-1}$ ) the diffusion coefficient of Nb(V) ( $D_{\text{Nb(V)}} = 8.5 \times 10^{-5} \text{ cm}^2 \text{ s}^{-1}$ ) is 2.7 times higher. Thus the residual concentration of the fluoro complexes must be higher or the ligand displacement is not complete. The backward calculation using the value of diffusion coefficient for the system without oxide ions shows that only ca. 70 % of added oxide amount was consumed by the fluoro complex displacement reaction. Free oxide ions in the melts reacted with available mono-oxyfluoro complexes to form di-oxyfluoro complexes.

Fig. 6 illustrates graphically the change of the diffusion coefficient value of the niobiumfluoro complex with changing  $n_{\text{O}}:n_{\text{Nb}}$  ratio in the  $\text{LiF-NaF-K}_2\text{NbF}_7\text{-Na}_2\text{O}$  melts at  $750^\circ\text{C}$ . With the  $n_{\text{O}}:n_{\text{Nb(V)}}$  ratio up to 0.7 there is no change in the diffusion coefficient of the mono-oxyfluoro complex. The coefficient

**Table 1.** Chronopotentiometric Data Obtained Using Platinum Working Electrode at the Reduction of  $K_2NbF_7$  in LiF—NaF Eutectic Melts with Various Amounts of  $Na_2O$  Added at 750°C

$c^o(Nb(V))$ mol m <sup>-3</sup>	$n_O:n_{Nb(V)}$	$\alpha$	$c(Nb(V))$ mol m <sup>-3</sup>	$c(Nb(V),O)$ mol m <sup>-3</sup>	$j$ A m <sup>-2</sup>	$(E_1)_{\tau/4}$ V	$\tau_1$ s	$D_{Nb(V)} \cdot 10^5$ cm <sup>2</sup> s <sup>-1</sup>	$(E_2)_{\tau/4}$ V	$\tau_2$ s	$D_{Nb(V),O} \cdot 10^5$ cm <sup>2</sup> s <sup>-1</sup>
57.1	0	—	—	—	667	-1.02	4.15	3.2	—	—	—
70.3	0.23	0.64	59.9	10.4	1203	-1.02	1.42	3.2	-1.27	0.27	0.9
70.3	0.23	0.72	58.7	11.6	1157	-1.04	1.46	3.2	-1.23	0.29	1.1
70.3	0.23	0.72	58.7	11.6	1018	-1.03	1.90	3.2	-1.23	0.37	0.7
70.3	0.62	0.72	38.9	31.4	1110	-1.05	0.70	3.2	-1.26	0.85	1.1
113.9	0.67	0.72	59.2	54.7	1296	-0.91	1.78	3.2	-1.18	1.97	1.4
113.9	0.67	0.69	61.2	52.7	1111	-0.90	1.71	3.2	-1.21	2.56	1.4
70.3	0.68	0.70	36.8	33.5	1296	-0.99	0.50	3.2	-1.24	0.86	1.7
70.3	0.68	0.67	38.3	32.0	1481	-1.02	0.35	3.3	-1.26	0.64	1.9
38.3	0.8	0.69	17.1	20.8	1481	-0.98	0.08	3.2	-1.24	0.37	4.7
38.3	0.8	0.71	16.5	21.3	1296	-1.03	0.09	3.2	-1.28	0.48	4.2
64.7	1	0.70	19.2	45.5	1481	-0.98	0.10	3.2	-1.28	0.79	2.3
64.7	1	0.70	19.4	45.3	926	-1.03	0.26	3.2	-1.32	2.06	2.4

$c^o(Nb(V))$  – initial concentration of  $K_2NbF_7$ ;  $\alpha$  – degree of niobiumfluoro complexes to mono-oxyfluoro complexes conversion.



**Fig. 6.** Change in the diffusion coefficient of niobiumoxyfluoro complex against  $n_O:n_{Nb(V)}$  ratio in LiF—NaF— $K_2NbF_7$ — $Na_2O$  melts at 750°C.

increases in the ratio interval 0.7—0.9 and then again decreases. The increase in the diffusion coefficient of the mono-oxyfluoro complex could be explained by the transition of the  $[Nb(V)OF_5]^{2-}$  complex to the  $[Nb(V)OF_6]^{3-}$  one in the melts, which causes the concentration change of electroactive species in the melt. With regard to the diffusion coefficient values in the melts with the ratio up to 0.7, the fluoro complexes undergo the deposition process. Coherent and dense deposit is expected. With the ratio up to 0.9 the mono-oxyfluoro complexes become more active. The presence of oxygen in the structure of the complex decreases its symmetry thus facilitating the deposition process resulting in the fact that a nonmetal deposit could be obtained as well.

## CONCLUSION

In the presence of oxide ions in fluoride melts niobiumoxyfluoro complexes are formed. At low concentration of oxygen mono-oxyfluoro complexes have the form of  $[Nb(V)OF_5]^{2-}$ . With the  $n_O:n_{Nb(V)}$  ratio higher than 0.7 the complex changes to the  $[Nb(V)OF_6]^{3-}$  one. The ligand displacement of the niobiumfluoro complexes to the mono-oxyfluoro complexes is not complete and the conversion degree was found to be 0.7. Due to free oxide ions in the melt di-oxyfluoro complexes are formed and they coexist with mono-oxyfluoro complexes despite the low concentration of oxide ions in the melt. The diffusion coefficient of oxyfluoro complexes in fluoride melts depends on the  $n_O:n_{Nb(V)}$  ratio in the melts. With the  $n_O:n_{Nb(V)}$  ratio up to 0.7 there is no change in the diffusion coefficient of the mono-oxyfluoro complex. The coefficient strongly increases in the ratio interval 0.7—0.9 and then again decreases.

*Acknowledgements.* The present work was financially supported by the Scientific Grant Agency of the Ministry of Education of the Slovak Republic and the Slovak Academy of Sciences under the No. 2/4032/97.

## REFERENCES

1. Sakawa, M. and Kuroda, T., *Denki Kagaku* 236, 146 (1968).
2. Van, V., Silný, A., Híveš, J., and Daněk, V., *Electrochem. Commun.* 1, 295 (1999).
3. Daněk, V., Chrenková, M., and Silný, A., *Coord. Chem. Rev.* 167, 8 (1997).
4. Keller, O. I., *Inorg. Chem.* 2, 783 (1963).
5. Barner, J. H., Christensen, E., Bjerrum, N. J., and Gilbert, B., *Inorg. Chem.* 30, 561 (1991).

6. Fordyce, J. S. and Baum, R. L., *J. Chem. Phys.* 44, 1166 (1966).  
 7. Peacock, R. D. and Sharp, D. W. A., *J. Chem. Soc.* 1959, 2762.  
 8. Brown, D., *J. Chem. Soc. A* 1964, 4944.  
 9. Field, B. O. and Hardy, C. J., *Proc. Chem. Soc.* 1963, 11.  
 10. Pausewang, G. and Rudorf, W., *Z. Anorg. Allg. Chem.* 69, 364 (1969).  
 11. Van, V., Silný, A., and Daněk, V., *Electrochem. Commun.* 1, 354 (1999).

The flow rate both at deposition and stripping was set constant in the range of 0.2 to 0.5 cm<sup>3</sup> min<sup>-1</sup>. The built-in reference electrode was used as an Ag/AgCl reference electrode. The counter electrode was a Pt mesh electrode. Throughout this paper all potentials are referred to the Ag/AgCl reference electrode.

The high-pressure sample digestion device (Bergström, Malmö, Sweden) with 50 cm<sup>3</sup> PTFE vessels was used. Digestion was performed in a two-step process using a microwave digestion system (Pachomat, Wrocław, Poland). The digestion was performed by low-through stripping cathodic voltammetry (LSCV) with a scan rate of 10 mV s<sup>-1</sup>. The stripping potential was set at -0.5 V vs. Ag/AgCl. The stripping current was measured with a 100 pA sensitivity. The stripping time was 10 s. The stripping potential was set at -0.5 V vs. Ag/AgCl. The stripping current was measured with a 100 pA sensitivity. The stripping time was 10 s.

High-Pressure Digestion

EXPERIMENTAL

The samples were digested in a high-pressure digestion vessel (Pachomat, Wrocław, Poland) with a microwave digestion system (Pachomat, Wrocław, Poland). The digestion was performed by low-through stripping cathodic voltammetry (LSCV) with a scan rate of 10 mV s<sup>-1</sup>. The stripping potential was set at -0.5 V vs. Ag/AgCl. The stripping current was measured with a 100 pA sensitivity. The stripping time was 10 s.

The electrode was plated with gold at the beginning of the experiment. The stripping potential was set at -0.5 V vs. Ag/AgCl. The stripping current was measured with a 100 pA sensitivity. The stripping time was 10 s.

The parameters of the instrument were set as follows: deposition potential 200 V, stripping potential 0 V, scan rate 10 mV s<sup>-1</sup>, and stripping time 10 s. The stripping potential was set at -0.5 V vs. Ag/AgCl. The stripping current was measured with a 100 pA sensitivity. The stripping time was 10 s.

The stripping potential was set at -0.5 V vs. Ag/AgCl. The stripping current was measured with a 100 pA sensitivity. The stripping time was 10 s.